Design of a Microwave Assisted Discharge Inductive Plasma Accelerator

Ashley K. Hallock*

Princeton University, Princeton, NJ, 08544

Kurt A. Polzin[†]

NASA - Marshall Space Flight Center, Huntsville, AL 35812

The design and construction of a thruster that employs electrodeless plasma preionization and pulsed inductive acceleration is described. Preionization is achieved through an electron cyclotron resonance discharge that produces a weakly-ionized plasma at the face of a conical theta pinch-shaped inductive coil. The presence of the preionized plasma allows for current sheet formation at lower discharge voltages than those employed in other pulsed inductive accelerators that do not employ perionization. The location of the electron cyclotron resonance discharge is controlled through the design of the applied magnetic field in the thruster. Finite element analysis shows that there is an arrangement of permanent magnets that yields a small volume of resonant magnetic field at the coil face. Preionization in the resonant zone leads to current sheet formation at the coil face, which minimizes the initial inductance of the pulse circuit and maximizes the potential electrical efficiency of the accelerator. A magnet assembly was constructed around an inductive coil to provide structural support to the selected arrangement of neodymium magnets. Measured values of the resulting magnetic field compare favorably with the finite element model.

Nomenclature

$\mathbf{B}, B, B_r, B_z$	magnetic field (T)		m_e	elecetron mass (kg)
c	speed of light (m/s)		n_e	electron number density (m^{-3})
e	elementary charge (C)		ϵ	permittivity of free space (F/m)
$\mathbf{f}, f_r, f_z$	Lorentz body force density (N/m^2)		η	efficiency (%)
$\mathbf{j}, j_\theta$	current density (A/mm^2)		ω	wave frequency (rad/s)
k	wave vector (m^{-1})		ω_c	electron cyclotron frequency (rad/s)
ΔL	change in circuit inductance (H)		ω_p	plasma frequency (rad/s)
L_0	circuit or parasitic inductance, (H)		ω_{UH}	upper hybrid frequency (rad/s)

I. Introduction

IT is desirable to extend the lifetime and increase the reliability of an in-space propulsion system as much as possible due to the fact that maintenance or replacement of that system becomes particularly challenging once it has been launched into orbit from the surface of the Earth. In addition, the amount of payload as a percentage of the total vehicle mass can be increased if the size and mass of the propulsion system, including the propellant required to complete a mission, can be reduced. The use of electric propulsion (EP) reduces the amount of propellant needed for a given mission because of the high values of specific impulse associated with EP as compared to other conventional propulsion systems.

*Graduate Student, Mechanical and Aerospace Engineering Department, E-Quad Olden St. Princeton, NJ 08544, Student Member AIAA.

[†]Propulsion Research Engineer, Propulsion Research and Technology Applications Branch,Propulsion Systems Department, Senior Member AIAA.

American Institute of Aeronautics and Astronautics

Pulsed inductive plasma thrusters[1–3] are spacecraft propulsion devices in which electrical energy is capacitively stored and then discharged through an inductive coil. The thruster is electrodeless, with a time-varying current in the coil interacting with a plasma covering the face of the coil to induce a plasma current. Propellant is accelerated and expelled at a high exhaust velocity ($\mathcal{O}\,(10 - 100\ \text{km/s})$) by the Lorentz body force arising from the interaction of the magnetic field and the induced plasma current.

Thrusters of this type possess many demonstrated and potential benefits that make them worthy of continued investigation. The electrodeless nature of these thrusters eliminates the lifetime and contamination issues associated with electrode erosion in conventional electric thrusters. Also, a wider variety of propellants are available for use when compatibility with metallic electrodes in no longer an issue. Pulsed inductive accelerators have been successfully operated using propellants like ammonia, hydrazine, and CO_2, and there is no fundamental reason why they would not operate on other propellants like H_2O. It is well-known that pulsed accelerators can maintain constant specific impulse I_{sp} and thrust efficiency η_t over a wide range of input power levels by adjusting the pulse rate to maintain a constant discharge energy per unit pulse. It has also been demonstrated that a dynamically impedance-matched pulsed inductive thruster can operate in a regime where η_t is relatively constant over a wide range of I_{sp} values. Thrusters in this class have operated at high energy per pulse, and by increasing the pulse rate they offer the potential to process very high levels of power using a single thruster.

The capacitors in some inductive accelerators, like the Pulsed Inductive Thruster (PIT) [1, 2, 4], must be charged to high voltages so that the discharge through the inductive coil can first ionize the propellant. One way to alleviate this high voltage requirement is to partially ionize the propellant in front of the inductive coil such that the induced electric field only needs to perform an under-voltage breakdown of already partially-ionized propellant[5], allowing for a lower initial voltage level on the energy storage system. Not all of the propellant must be preionized because only the preionized propellant within a few characteristic length scales of the inductive coil has any significant interaction with fields induced by the high-current pulse. The use of preionization is ubiquitous throughout the literature on pulsed inductive devices with a wide range of applications including plasma fusion and space propulsion. For example, preionization has been successfully employed by striking a discharge between two electrodes [6, 7], sending a separate lower-energy pulse through an inductive coil[8, 9], and creating a "seed" plasma [4, 10].

In this paper, we present a pulsed inductive accelerator concept called the Microwave Assisted Discharge Inductive Plasma Accelerator (MAD IPA), shown in Fig. 1, that employs an electron cyclotron resonance (ECR) discharge to preionize the propellant. A static magnetic field in the thruster, provided by permanent magnets, is designed so the ECR-driven discharge is located on the face of the inductive coil, only preionizing the propellant in the region where the coil can interact with it. The rest of this paper describes the design of the pulse circuit, inductive coil, and ECR ionization system of the MAD IPA, and their subsequent incorporation into a pulsed inductive plasma accelerator.
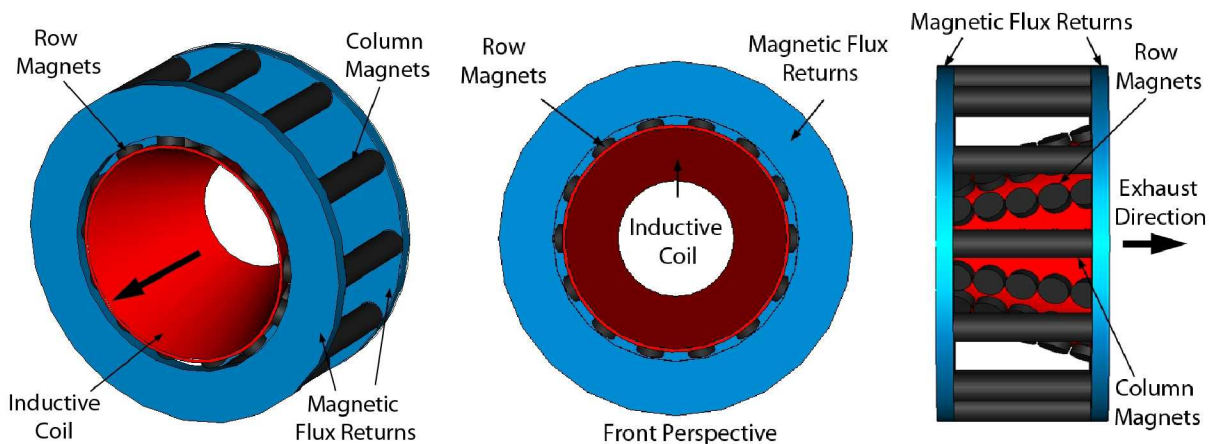

Figure 1. Finite element model of the Mad IPA, with the inductive coil shown in red, the permanent magnets in gray, the ferrite pieces in green, and the thruster axis as a black arrow.

American Institute of Aeronautics and Astronautics

II. Pulse Circuit

The pulse circuit for the MAD IPA consists of a capacitor assembly and a low-inductance triggered spark gap switch. Four 10 μF, 4kV capacitors are connected in parallel and discharged using a PerkinElmer low-inductance triggered spark gap switch designed to operate with an applied voltage from 2-4 kV. This voltage range yields a bank energy per pulse between 160-640 J. The trigger electrode of the spark gap is connected to a pulser circuit that uses a 70:1 transformer connected to a smaller capacitor with a low charging voltage ($\mathcal{O}\,(100 \text{ V})$), which yields a high voltage ($\mathcal{O}\,(10 \text{ kV})$) pulse on the secondary side of the transformer when the low-voltage circuit is triggered. Discharge of the spark gap, and subsequently the main capacitor bank, is achieved by introducing the high-voltage pulse to the spark gap trigger electrode. The cathode of the spark gap switch, the main capacitor bank, and the pulser circuit are all grounded at a single, common point. Eight coaxial cables connected in parallel to the main capacitor bank assembly feed current to the inductive coil. Representative waveforms showing the total current in the unloaded (with no plasma present) inductive coil as a function of time for two different capacitor bank charging voltages are shown in Fig. 2.
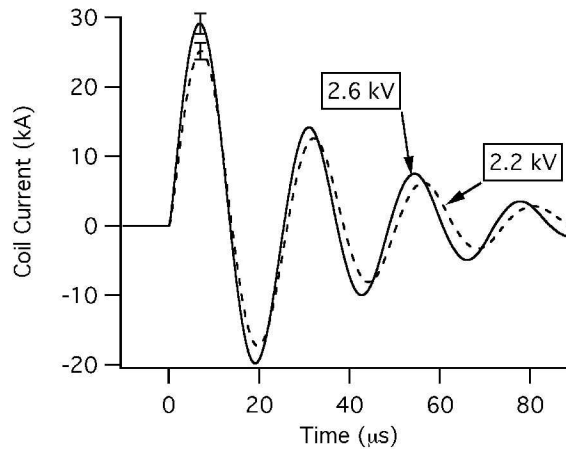

Figure 2. Total current in the inductive coil (with representative error bars) as a function of time for different charging voltages on the capacitor assembly.

III. Inductive Coil

The inductive coil, shown in Fig. 3, is in the shape of a conical theta pinch and is composed of spiral copper traces 0.2 mm thick that cover both sides of a 0.45 mm thick mylar conical frustum. The conical frustum has a minor radius of 4 cm, a length of 10 cm, and a half cone angle of 20°. An additional layer of mylar with a black protective coating is added to the inner surface of the frustum to insulate the inner copper traces from the plasma. The pattern of the copper traces, shown in Fig. 4, is such that the radial and axial components of current from the two sides of the mylar will cancel, yielding a uniform, azimuthal current at the coil face (as in the PIT [1]). Currrent is fed to each trace individually via coaxial cables connected in parallel at the upstream end, or smaller end, of the cone. Each current trace follows an Archimedes spiral, completing two full turns while traveling along the entire axial length of the frustum twice before the path returns to the point of origin on the opposite side of the mylar insulation. The inductance of the coil is 426 nH as measured using an Agilent 4285A precision LCR meter.

IV. Preionization

An ECR preionization scheme was chosen to produce a thin layer of plasma on the interior surface of the conical-shaped inductive coil because it offers the unique ability to control the location of ionization electrodelessly and without the imposition of high voltage-requirements, advantages of ECR that have previously been demonstrated in the Electrodeless Plasma Thruster [11–13]. Inductively-coupled current sheet formation at low discharge voltages (1-4 kV) requires only a thin layer of preionized plasma. As the current
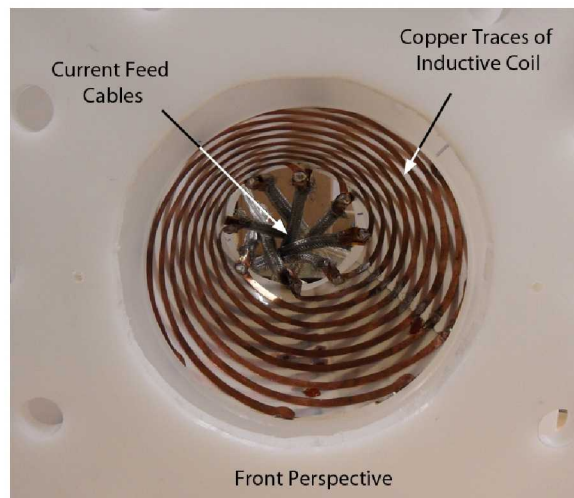
American Institute of Aeronautics and Astronautics

Figure 3. The inductive coil, composed of copper traces adhered to a mylar sheet that provides insulation and structural support, is shown in the thruster with the magnets, magnetic flux returns, and black protective sheet on the coil face removed. The eight coaxial cables that feed current to the copper traces are visible through the open center of the thruster.
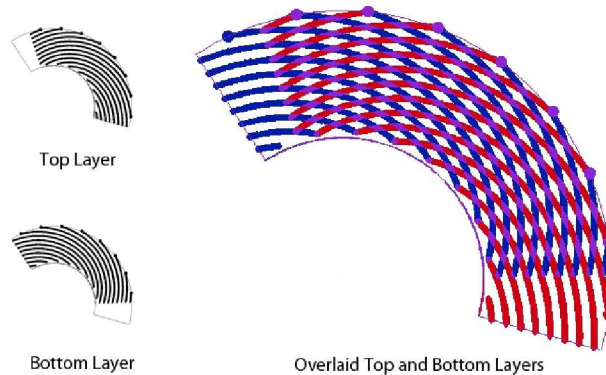

Figure 4. Copper trace design used to create the conical inductive coil. The top layer is shown in red, the bottom layer in blue, and where they are superposed in purple.

sheet forms and is inductively accelerated, the external circuit inductance will change from an initial value L_0 to a final value $L_0 + \Delta L$. It is well known that the value of the ratio $\Delta L/L_0$ must be large for efficient electromagnetic acceleration of a gas [14]. This ratio is maximized when the preionized plasma forms as close to the inductive coil as possible, but it should not form so closely that it causes insulator ablation. In the remainder of this section we describe the subsystems required to support an ECR discharge capable of satisfying these requirements.

A. ECR Energy Addition Using Microwaves

In the ECR process, energy is transferred from an electromagnetic (EM) wave to the electrons in the plasma. The wave energy can be focused into a given part of the plasma if a resonant condition can be established. The resonance condition can be determined by setting the wave number k equal to zero in the dispersion relation for the wave and solving for the frequency ω of the wave. Of the four principal waves that propagate in a magnetized plasma, only the extraordinary wave (X wave) and the right-hand polarized wave (R wave) are capable of significant energy exchange with electrons in the plasma.

    The X wave is defined as a wave where both the wave vector and the electric field component of the wave

are perpendicular to the applied magnetic field B. The X wave dispersion relation is

$$\frac{c^2 k^2}{\omega^2} = 1 - \frac{\omega_p^2}{\omega^2}\left[\frac{\omega^2 - \omega_p^2}{\omega^2 - \omega_{UH}^2}\right], \tag{1}$$

where c is the speed of light. The plasma frequency ω_p is defined as

$$\omega_p = \frac{n_e e^2}{\epsilon_0 m_e} \tag{2}$$

where n_e is the electron number density, e is the charge on an electron, ϵ_0 is the permittivity of free space, and m_e is the mass of an electron. The upper hybrid frequency ω_{UH} is given as

$$\omega_{UH} = \left(\omega_p^2 + \omega_c^2\right)^{\frac{1}{2}}, \tag{3}$$

where ω_c is the electron cyclotron frequency:

$$\omega_c = \frac{eB}{m_e}. \tag{4}$$

Resonance for the X wave occurs at $\omega = \omega_{UH}$, a condition that causes the right hand side of Eq. 1 to equal infinity.

The R wave is defined as having $k \parallel B$ with an electric field component that is perpendicular to B and rotates around B in the same sense as the electrons in the plasma. The dispersion relation for R waves is:

$$\frac{c^2 k^2}{\omega^2} = 1 - \frac{\omega_p^2/\omega^2}{1 - \omega_c/\omega} \tag{5}$$

Resonance for this wave occurs when $\omega = \omega_c$ which, unlike the X wave resonance, depends only upon the value of B. It is this resonance that we target in the MAD IPA, controlling the preionized plasma location solely through design of the background magnetic field profile. It should be noted that, regardless of the polarization of the EM waves launched into the plasma, R waves will form and propagate in the plasma in response to any launched waves whose wave vector is mostly aligned with the background magnetic field. In general, the restriction of wave emission to a single polarization has been shown to provide no benefit [15]. In our ECR scheme, this should hold true due to the fact that any waves in the plasma that do not propagate as R waves have a certain probability of being transformed into R waves through reflections with one of the metallic surfaces of the inductive coil. Therefore, no attempt was made in the design of the EM wave delivery system to control the polarization of the waves.

In the present MAD IPA experiment, waveguides carry microwave energy from a magnetron source through a waveguide pressure window to a wave-launcher that feeds microwaves to the interior volume contained by the conical inductive coil. Waveguides were employed due to the low power levels (as low as 100 Watts) at which coaxial microwave cables have been known to arc [13], allowing for testing over a wider range of ECR input power levels. While only the TE_{10} mode propagates through the rectangular waveguide sections, once the wave transitions to the cylindrical, coaxial wave-launcher, all field polarization is lost. The waves are emitted with a random orientation from the end of the launcher into the volume enclosed by the inductive coil.

In future engineering and flight units, the magnetron and waveguide system could be replaced by surface-mount microwave resonator circuits (not unlike those commonly found inside cell phones) placed along the inside of the inductive coil. The signal from these circuits could be amplified if needed to provide a level of preionization sufficient to allow inductive current sheet formation for a particular pulse energy and capacitor bank charging voltage. Another advantage to this design is that the EM waves travel radially towards the thruster axis across a background magnetic field that decreases in magnitude at smaller radii, preventing wave reflections that might have otherwise occurred before the wave reached the location for resonance interaction. The only disadvantage to this design would be the addition of microwave circuits (and associated insulation) between the inductive coil traces and the plasma, slightly increasing the distance between the initial current sheet and the inductive coil, leading to an increased L_0.

B. Applied Magnetic Field Design

The applied magnetic field can be produced using electromagnetic coils, permanent magnets, or a combination of the two. Permanent magnets were chosen for MAD IPA due to the additional weight and power penalties associated with the use of electromagnetic coils.

The resonance value for the applied magnetic field can be found by equating the electron cyclotron frequency, defined in Eq. 4, to the frequency of the EM waves. For an EM wave with a frequency of 2.45 GHz, the resonant magnetic field value is about 0.0875 T. Therefore the applied magnetic field profile should be designed such that the absolute value of the field is equal to this value only in the space directly in front of the inductive coil, with a rapid decrease in B in the direction normal to the surface of the coil toward the interior of the thruster. The resonance zone should also not intersect the inductive coil to help keep the plasma from interacting with and ablating the insulating surface in front of the inductive coil. In locations where the magnetic field bends towards or intersects the inductive coil, the field strength should be great enough to reflect, or magnetically mirror, the preionized plasma away from the surface.

The direction of the magnetic field should also parallel that of the self magnetic field created by the plasma current, increasing the Lorentz body force density $\mathbf{f}$ that accelerates the propellant, which is related to both the plasma current density $\mathbf{j}$ and the magnetic field $\mathbf{B}$:

$$\mathbf{f} = \mathbf{j} \times \mathbf{B}. \tag{6}$$

This equation can be separated into an axial and a radial component:

$$f_z = j_\theta B_r \qquad \text{and} \qquad f_r = j_\theta B_z \tag{7}$$

With a properly contoured magnetic field profile, the permanent magnet assembly not only creates an ECR zone but also contributes to the axial and radial acceleration of plasma. However, if the magnetic field intersects the inductive coil it may partially cancel the induced magnetic field at that location, reducing the achievable thrust. In addition, if there is not enough magnetic mirroring to repel the plasma from the coil surface, the insulator may be ablated by the preionized propellant.
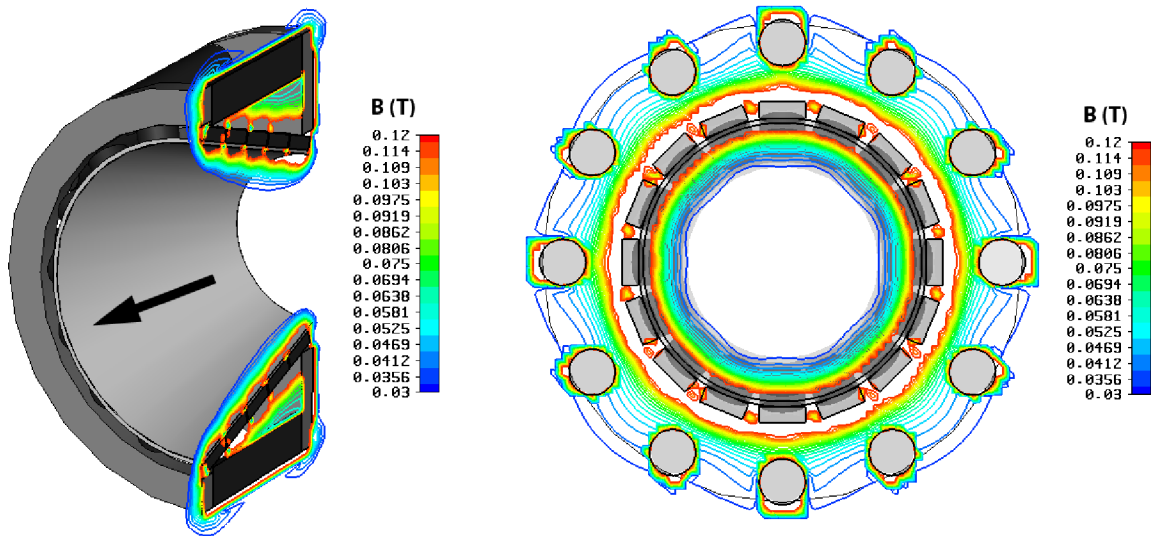

Figure 5. Finite element model of the magnetic field surrounding the Mad IPA, with the resonance zone shown in yellow, green and light blue, and the thruster axis as a black arrow. The structure is shown in black and white to clarify the magnetic field contour. *Left*: Perspective view. *Right*: Front view along thruster axis.

The desired magnetic field is produced in the following manner. First, axially-oriented columns of disk magnets bounded at their ends by ferrite discs create a relatively uniform magnetic field profile within the volume of the inductive coil that follows the geometry of the cone with minimal intersection points. This field has a value that is roughly half of the resonant value and is oriented such that it may enhance the thrust. Next, additional disc magnets are laid flat in rows on the outer surface of the inductive coil to create

American Institute of Aeronautics and Astronautics

a magnetic field that has a large gradient where the magnitude quickly decreases when moving radially inward towards the thruster axis. While this field is mostly azimuthal, and will not contribute to thrust, the superposition of this field with that of the column magnets creates a profile where the magnitude of the magnetic field close to the inductive coil is at resonance. The radially-inward gradient of the field is such that its value is roughly half the resonant value only a few mm away from the inductive coil. The magnet assembly, finite element model, and simulation results are shown in Fig. 5.
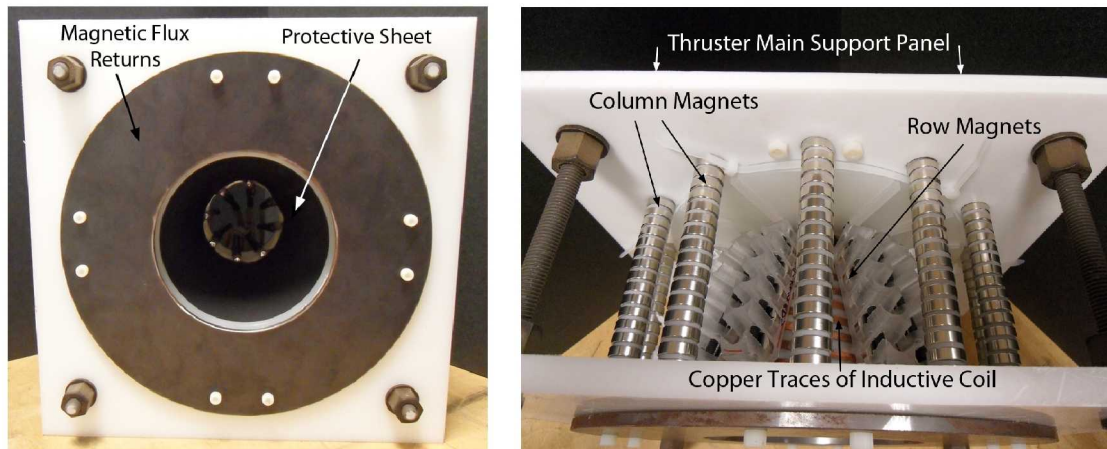
C.   Assembled Unit

Figure 6. Photograph of the MAP IPA shown from the *Left:* front, and *Right:* top.

Neodymium-52 disc magnets, 0.25 in thick with a diameter of 0.75 in, were used to produce the applied magnetic field. Only non-conductive material was used to construct the supporting structure that holds the magnets in place around the inductive coil. Row magnets are held in place inside plexiglas blocks, where each block contains five channels into which disc magnets can be inserted. Fourteen of these blocks were placed at even intervals around the inductive coil to create the pattern of disc magnets used in the magnetic field finite element analysis model. Once the row magnets were in place, twelve columns of nineteen magnets each were azimuthally-spaced around the inner assembly. These columns are supported by slots in the thruster main support panels, and are held in place by two steel discs that serve as the magnetic flux returns. Photographs of the thruster and its magnet support assembly are shown in Fig. 6. The inductive coil is hidden from view in the left panel of Fig. 6 by a black protective sheet, but it is visible from the outside in the right panel. The eight coaxial cables that feed current to the copper traces of the inductive coil can be seen through the open center of the thruster in the left panel.

Values of the magnetic field produced by the magnet assembly were measured at multiple locations over grids in the r-z plane at multiple azimuthal locations using a Lakeshore 421 gaussmeter. Due to the large radial gradient in magnetic field strength at the inner surface of the inductive coil, measurements were highly location-sensitive, with the field strengths varying by hundreds of Gauss over a distance of 1 mm. The values in the contour plot shown in Fig. 7 exhibit ECR resonance zone very near the coil face, comparing favorably with the simulation results shown in Fig. 5.

V.   Conclusions

We presented an electrodeless plasma accelerator concept, the MAD IPA, that uses an ECR preionization scheme to produce a seed plasma that is further ionized and accelerated by current pulsed through an inductive coil. The current rise rate (inductive voltage drop) needed across the inductive coil during a pulse is lower when preionization is employed since the inductive coil is not required to breakdown a neutral gas. This allows for a lowering of the charge voltage and commensurate discharge energy per pulse in the MAD-IPA relative to other pulsed inductive concepts like the PIT. ECR was chosen to produce the preionized plasma because the location of the resonance region is controllable through the applied magnetic field design. Through finite element analysis it was determined that an arrangement of permanent magnets
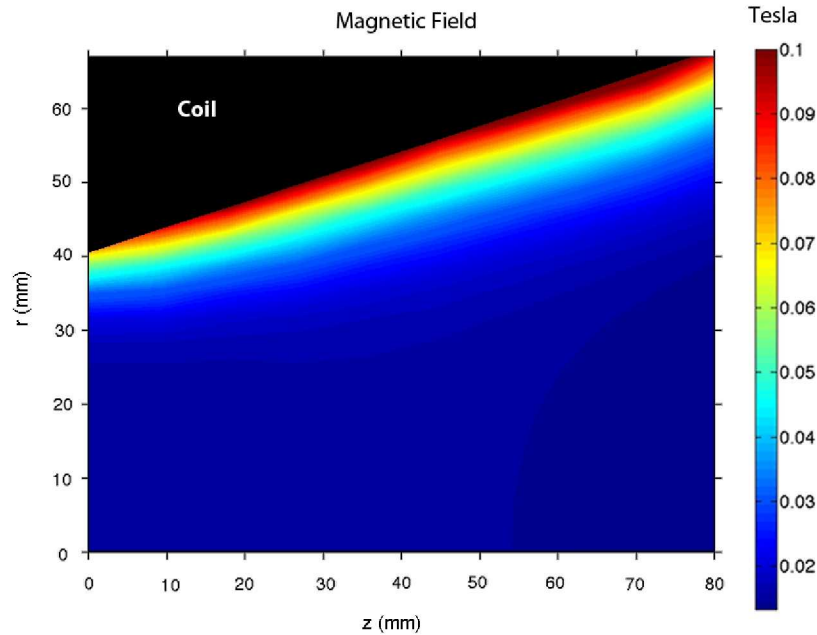
American Institute of Aeronautics and Astronautics

Figure 7. Measured magnetic field created by an arrangement of permanent magnets. The contour is of an r-z plane bounded axially by the edges of the inductive coil, and bounded radially by the surface of the inductive coil and the centerline of the thruster.

could be employed to produce a magnetic field topology that satisfied the design requirements of the MAD IPA. A supporting structure was constructed around an inductive coil to hold hundreds of neodymium magnets in the correct positions as indicated by the model. Measurements of the resulting magnetic field compare favorably with the modeling results, indicating a thin zone at the inductive coil face that should support an ECR discharge.

Acknowledgments

References

[1]Dailey, C. L. and Lovberg, R. H. The PIT MkV Pulsed Inductive Thruster. Technical Report 191155, Lewis Research Center, Redondo Beach, CA, July 1993.

[2]Lovberg, R. H. and Dailey, C. L. A PIT primer. Technical Report 005, RLD Associates, Encino, CA, 1994.

[3]Polzin, K. A. *Faraday Accelerator with Radio-frequency Assisted Discharge (FARAD)*. Ph.D. dissertation, Princeton University, Department of Mechanical and Aerospace Engineering, 2006.

[4]Choueiri, E. Y. and Polzin, K. A. Faraday Acceleration with Radio-frequency Assisted Discharge. *Journal of Propulsion and Power*, 22(3):611–619, May-June 2006.

[5]Polzin, K. A. Scaling and System Considerations in Pulsed Inductive Plasma Thrusters. *IEEE Transactions on Plasma Science*, 36(5):2189–2198, October 2008.

[6]Josephson, V. and Hales, R. W. Parametric Study of the conical Shock Tube. *The Physics of Fluids*, 4(3):373–379, 1961.

[7]Cassibry, J. T. Fimognary, P. J. and Ims, K. E. Effects of Pre-ionization and Bias Field on Plasmoid Formation and Acceleration. Number AIAA-2007-5262, July 2007.

[8]Josephson, V. Production of High Velocity Shocks. *Journal of Applied Physics*, 29(1):30–32, 1958.

[9]Cruddace, R. C. and Hill, M. Mechanism of Plasma Acceleration in a Conical Theta-pinch Gun. Technical Report CLM-M52, Culham Laboratory, 1966.

[10]Miller, R. Best, S Ownes, T. Polzin, K. A., Rose, F. M. and Dankanich, J. Design of a Low-Energy FARAD Thruster. Number AIAA 2007-5257, July 2007.

[11]Emsellem, G. D. and Larigaldie, S. Development of the Electrodeless Plasma Thruster at High Power: Investigation of the Microwave-Plasma Coupling. Number IEPC-2007-240, September 2007.

[12]Emsellem, G. D. and Larigaldie, S. Low Power Behavior of the Electrodeless Plasma Thruster. Number AIAA-2008-5009, July 2008.

[13]Emsellem, G. D. Coupling and Erosion Evaluation of the High Power Electrodeless Plasma Thruster at Low Power at Princeton University. Number AIAA-2009-5449, August 2009.

[14]Gooding, T. Lovberg, R. H., Hayworth, B. R. The Use of a Coaxial Gun for Plasma Propulsion. Technical Report AE62-0678, G. D. Convair, 1962.

[15]Geller, R. *Electron Cyclotron Resonance Ion Sources and ECR Plasmas.* Institute of Physics Publishing, 1996.